Effects of salt addition on strength and dynamics of hydrophobic interactions

Fujita, Takatoshi
Watanabe, Hirofumi
Tanaka, Shigenori

(Citation)
Chemical Physics Letters,434:42-48

(Issue Date)
2007-01

(Resource Type)
journal article

(Version)
Accepted Manuscript

(URL)
https://hdl.handle.net/20.500.14094/90000598

Effects of salt addition on strength and dynamics of hydrophobic interactions

Takatoshi Fujita [a,c], Hirofumi Watanabe [b,c], Shigenori Tanaka [a,b,c,*]

[a] *Faculty of Human Development, Kobe University, 3-11 Tsurukabuto, Nada, Kobe 657-8501, Japan*

[b] *Graduate School of Science and Technology, Kobe University, 1-1 Rokkodai, Nada, Kobe 657-8501, Japan*

[c] *CREST, Japan Science and Tehnology Agency, 4-1-8 Honcho, Kawaguchi, Saitama 332-0012, Japan*

Abstract

Effects of salt addition on strength and dynamics of hydrophobic interactions are investigated by molecular dynamics simulations for hydrophobic solutes in aqueous solution of various salts such as sodium chloride, ammonium chloride, and guanidinium chloride. Hydrophobic interaction is reduced by ammonium chloride, enhanced by sodium chloride, and strongly enhanced by guanidinium chloride. Addition of salts tends to delay the relaxations of hydrophobic associations by reducing water diffusivities and enhancing structuring of water. The underlying molecular mechanisms are discussed in detail.

1 Introduction

Hydrophobic effects are observed in many important biological phenomena. For instance, hydrophobic interaction is one of the major driving forces in protein folding [1-4]. Hydrophobic interactions consist of a direct interaction between the nonpolar groups and indirect effects of aqueous solutions. Although water is a dominant component, numerous other molecules are also present in these solutions. The subjects of salt, cosolvent and other additive effects on biological molecules have been reviewed in the literature [5-7]. The

* Corresponding author. Fax: +81-78-803-7761
Email address: tanaka2@kobe-u.ac.jp (Shigenori Tanaka).

key factors for understanding their effects on biological molecules are associated with the hydrophobic effects.

The effects of salts on solubility and hydrophobic hydration processes have often been studied using molecular theory and simulations [8-11]. However, salt or cosolvent effects on hydrophobic interactions have not yet been studied well except for some investigations [12-14]. Above all, the study by Ghosh *et al.* [12] was the first attempt to quantify the salt dependence of hydrophobic interactions. They interpreted salt dependence of hydrophobic interactions within the framework of preferential interactions by Timacheff [7].

The present study focuses on the dependence of hydrophobic interactions on salt species. The salts studied in this work are sodium chloride (NaCl), ammonium chloride (NH_4Cl), and guanidinium chloride (GdmCl). The salts studied here are associated with the Hofmeister series [5,6]; NH_4Cl brings about salting-out and stabilizing effects on peptides and proteins, and GdmCl produces salting-in and denaturing effects, while NaCl gives intermediate effects [5,6,15]. One of the goals of our study is to explore their underlying mechanisms.

Here we employ molecular dynamics (MD) simulations to investigate the salt dependence of hydrophobic interactions. We calculate the pair potential of mean force (PMF) between methanes as a quantitative measure of hydrophobic interactions. We focus on such effects of salts on hydrophobic interactions as the change in the PMF upon salt additions, and study their molecular mechanisms.

In order to fully understand the kinetics of dynamical processes such as protein folding, however, it is important to know the relaxation and lifetimes of hydrophobic associations [16]. Thus we also calculate the distinct part of van Hove function (DVH) between methanes. This DVH provides the comprehensive information on the dynamics of hydrophobic associations. We thus investigate the dynamical processes of hydrophobic associations and their salt dependence.

This paper is organized as follows: Computational details are shown in Section 2. In Section 3, we present the results obtained from MD simulations. Both strength and kinetics of hydrophobic interactions are changed by the addition of salts. Then structural features in each aqueous solution are presented. Further, we discuss the correlation between hydrophobic interactions and structural features in aqueous solutions. The main results are briefly summarized in the concluding Section 4.

2 Computational methods

We performed molecular dynamics (MD) simulations of methanes in aqueous solutions of various salts (NaCl, NH_4Cl, and GdmCl) using TINKER software [17]. The number and concentration of molecular species included in each simulation are given in Table 1. The molar concentrations of each salt were set at approximately 2 M for which the qualitative difference of salt additions becomes clear in a moderate way [12,15]. The TIP3P model for water [18], the OPLSAA models for the salt ions [19,20], and the spherically symmetric Lennard-Jones (LJ) model for methane molecules [12,21] were employed. Table 2 lists the LJ parameters and partial charges for all the species used in this study.

The Beeman algorithm [22] was used for the integration method. Periodic boundary conditions were applied and the particle mesh Ewald method [23] was used to calculate the long-range electrostatic interactions without cutoff. The Lennard-Jones potential contribution were cut off at 9 Å. A time step of 2 fs was employed, and Berendsen's coupling algorithm was used to maintain constant temperature [24] with a time constant for heat bath coupling being set at 0.5 ps. All the hydrogen atoms were constrained at their ideal positions using the RATTLE algorithm. All the systems were volume equilibrated at a pressure of 1 atm using Berendsen's pressure coupling algorithm with a pressure relaxation time of 0.5 ps. Equilibration runs of 1 ns were followed by production runs of 10 ns (at each system) in the NVT ensemble at the temperature $T = 300$ K. Configurations were saved every 0.5 ps for the following analysis.

3 Results and discussion

3.1 Salt effects on strength of hydrophobic interactions

In order to quantify the hydrophobic interactions we calculate methane-methane (Me-Me) potentials of mean force (PMF) defined by the following expression:

$$W(r) = -k_B T \ln g(r), \tag{1}$$

where $g(r)$ is the Me-Me radial distribution function in aqueous solutions and k_B is the Boltzmann constant. These PMFs provide a quantitative measure of the strength of hydrophobic interactions at the two-particle level.

Figure 1 shows the Me-Me PMF, and the changes in the Me-Me PMF upon salt addition relative to the PMF in pure water, $\Delta W(r) = W(r) - W_{\mathrm{None}}(r)$, obtained from MD simulations. As for the Me-Me PMF in pure water, the contact minimum (CM) is observed at ∼3.9 Å ($W = -3.3$ kJ/mol), and the solvent separated minimum (SSM) is observed at ∼7.4 Å ($W = -0.38$ kJ/mol), whereas desolvation barrier (BARR) appears between the two minima at ∼5.9 Å ($W = 0.86$ kJ/mol). These features of the PMF in pure water have been discussed in detail in the literature [25,26].

We are interested in the effects of salts on the hydrophobic interactions. As for the effects of salts on the Me-Me PMF, we have observed the stabilization by the addition of NaCl, the destabilization by NH_4Cl, and the stabilization by GdmCl which is stronger than by NaCl. The sensitivity of the PMF to salts depends on Me-Me separations, which we will describe later. These effects of salts are varied due to the salt species, which would be ascribed to the structures of their cations (*vide infra*).

The following features have been observed about the effect of NaCl on the Me-Me PMF, as seen in Fig. 1. The addition of NaCl have almost no effect on the location of CM, BARR, and SSM, which is different from the cases for NH_4Cl and GdmCl. The maximum stabilization occurs for the most compact Me-Me configuration, and the magnitude of change, $\Delta W(r)$, decreases monotonically with Me-Me separations. These features of the effect of NaCl on the Me-Me PMF are in agreement with the results obtained by Ghosh *et al.* [12].

The addition of NH_4Cl has a complex effect on the Me-Me PMF. The destabilization occurs for the short Me-Me separations corresponding to the CM and the BARR configurations, and the less destabilization occurs for the Me-Me separation of ∼9.0 Å, whereas the stabilization occurs for the SSM configuration. The maximum destabilization occurs at ∼5.1 Å ($\Delta W = 0.86$ kJ/mol), resulting in the inward movement of the BARR in the PMF.

The addition of GdmCl has the most dramatic effect on the Me-Me PMF among these salts. We observed the outward movement of the location of CM, BARR, and SSM. The maximum stabilization occurs between 4.2 and 5.1 Å ($\Delta W = -1.6$ kJ/mol), and the less stabilization occurs near ∼8.3 Å, while almost no change occurs for the Me-Me separation of ∼6.5 Å.

3.2 The dynamical procceses of methane-methane association and their salt dependence

In order to investigate the dynamics and the lifetime of Me-Me association, we calculated the Me-Me distinct part of van Hove correlation function (DVH),

defined by the following expression:

$$G_d(r,t) = \frac{1}{4\pi r^2 N} \left\langle \sum_{i,j}^{N} \sum_{i \neq j}^{N} \delta[r - |\mathbf{r}_i(0) - \mathbf{r}_j(t)|] \right\rangle. \quad (2)$$

This function provides the probability that at time t a methane is found at a distance r from an origin, given that another methane is located at the origin at the initial time, $t = 0$. At $t = 0$ the Me-Me DVH is proportional to the Me-Me radial distribudion function such as $G_d(r,t) = \rho g(r)$, whereas at long times and large separations the position of one methane is uncorrelated with the earlier position of another methane, $\lim_{r\to\infty} G_d = \lim_{t\to\infty} G_d = \rho = N/V$.

Figure 2 shows the Me-Me DVHs obtained from MD simulation. The striking features of these Me-Me DVHs are observed as follows: There are well developed peak at short time near $r = 0$, the height of which is larger than the average density. The height of this peak attains a maximum after a time τ_{max}, and then decreases again. This result indicates that once a methane has moved from the location it had at $t = 0$, there is a high probability that a different methane will occupy its location, and that this probability is the highest at the time, and then converges to the average density. We thus define the $\tau_{\max}$ as the time where the average value of G_d between 0 and 0.5 Å attains a maximum, $G_d^{\max}$ and evaluate the lifetime of Me-Me association, τ_{life}, as the time when its value first decreases to $(G_d^{\max} + \rho)/2$ after a maximum.

As for the Me-Me DVH in pure water, the $\tau_{\max}$ and the τ_{life} are 7 and 15 ps, respectively. The relaxation of hydrophobic association is considered to be long, compared to association driven by other interactions. For instance, as for the DVH between water molecules, e.g., the O-O DVH in pure water, first peak completely decays at 1 ps and the DVH converges to average density at 10 ps. In contrast to their relatively weak interactions, the lifetime of Me-Me association is long, which is considered as the characteristic feature of hydrophobic interactions; the association is mainly ascribed to the indirect effects of aqueous solutions. Further as a characteristic feature of Me-Me DVH, we have observed the developed peak at short time near $r = 0$, specific to the case of Me-Me DVHs. We have found that this characteristic feature of Me-Me DVHs is similar to that of glass forming liquids [27,28]. This similarity seems to be due to their slow relaxations.

The addition of salts tends to delay the relaxation of Me-Me association. The $\tau_{\max}$ and τ_{life} of each system are, 8 and 25 ps in NaCl solution, 47 and 75 ps in NH_4Cl solution, and 26 and 175 ps in GdmCl solution, respectively. The addition of NaCl has little effects on $\tau_{\max}$, while the additions of NH_4Cl and GdmCl increase the $\tau_{\max}$. The NH_4Cl causes the slower relaxation of the initial structure, as indicated by the behavior that the first and second peaks of DVH do not completely decay at 7 ps. The striking feature of the effect of GdmCl

is the higher peak near $r = 0$, the height of which is greater than the first maximum at $t = 0$.

3.3 Structural features in aqueous solutions and its correlation with methane-methane association

Figure 3 shows the water-water (O-O) and cation-water radial distribution functions (RDFs). From the O-O RDFs, the average water structure becomes more structured by the addition of GdmCl and NH_4Cl, as indicated by the strengthened peaks and dips, while the addition of NaCl leads to a slight change in O-O RDF. The coordination numbers of water around each cation are, 3.9 within 3.3 Å of Na^+ ion, 4.7 within 3.5 Å of a nitrogen atom of NH_4^+ ion, and 7.1 within 4.4 Å of a carbon atom of Gdm^+ ion. To see the dynamics of water, the diffusion constants of water molecules calculated from $D = \langle \Delta r^2(t) \rangle / 6t$ are, 5.3±2.1 in pure water, 5.0±1.8 in NaCl solution, 2.4±1.2 in NH_4Cl solution, and 2.8±1.7 in GdmCl solution in units of 10^{-5} cm^2/s, respectively. The addition of NaCl thus has little effect on water diffusivity, whereas the additions of NH_4Cl and GdmCl significantly decrease the water diffusivity. From these results, NH_4^+ and Gdm^+ ions are found to make water molecules around them well structured, resulting in the strengthened first peak in the O-O RDFs and the decreased diffusivity of water molecules, in contrast to the little effect of NaCl ions.

The first hydration shell of a Gdm^+ ion has a characteristic feature owing to the planar structure of a Gdm^+ ion (see the inset of Fig. 3 (d)). The average numbers of hydrogen-bonded water molecules per hydrogen atom of Gdm^+ ion is approximately 0.9 (within 2.4 Å of a hydrogen atom) from the H-O RDF in Fig. 3 (d), and thus there are approximately 5.4 hydrogen-bonded water molecules per Gdm^+ ion. On the other hand, the average hydration number of Gdm^+ ion is 7.1. These results indicate a tendency of relative deficiency (7.1−5.4=1.7) of hydrating water molecules directly above and below the plane of Gdm^+ ions, and the planar faces of Gdm^+ ion behave like hydrophobic surfaces. In contrast to the high density of the water molecules near the NH_2 group of Gdm^+ ion, the density of water molecules just above and below the planar faces of the Gdm^+ ion is low. This characteristic feature of a Gdm^+ ion has been noted previously by Mason *et al.* [29,30]. It is also noted that the use of Delunay-Voronoi tessellation method, which was not employed in the present study, would be another option for quantitative analysis.

Figure 4 shows the methane-water (Me-O) and methane-cation radial distribution functions (RDFs). As for the effects of salts on the first peak of the Me-O RDF, the slight enhancement by NaCl, the enhancement by NH_4Cl, and the reduction by GdmCl are observed. Preferential hydration and prefer-

ential dehydration are defined as cases where the height of first peak of Me-O RDF is higher or lower than that in pure water, respectively. Karla *et al.* [9] have found that preferential hydration leads to salting-out and preferential dehydration leads to salting-in of hydrophobic solutes in water. Our results support their findings; the salting-out ions (NH_4Cl, NaCl) lead to the preferential hydration and the salting-in ion (GdmCl) leads to the preferential dehydration.

The contact peak in the Me-Na^+ RDF is absent, below the average density, and smaller than the result by Ghosh *et al.* [12]. This difference seems to be due to the smaller value of Lennard-Jones ϵ parameter for Na^+ ions, and in our simulation there is almost no attraction between methanes and Na^+ ions.[1] The distribution of Na^+ ions near methane shows the strong depletion of these ions in the vicinal region relative to their density in the bulk. This preferential exclusion of Na^+ ions results from the favorable hydration of Na^+ ions, as shown by the high first peak of the Na^+-O RDF in Fig. 3 (b).

NH_4^+ ions show the favorable hydration in the same way as Na^+ ions, as seen in Fig. 3 (c). However, the contact peak appears in Me-NH_4^+ RDF in Fig. 4 (c), which is considered to be due to the van der Waals attraction between methanes and nitrogens. The NH_4^+ ions near methanes make water molecules around methanes well structured, resulting in the enhanced first peak in the Me-O RDF.

Among these ions, Gdm^+ ions interact most preferentially with methanes, as seen by the higher first peaks of the Me-Gdm^+ RDFs in Fig. 4 (d). As seen from the Me-Gdm^+ RDFs in Fig. 4 (d), in the average methane distribution around Gdm^+ ion, the methanes are located near the faces of planar Gdm^+ ions. This preferential interaction between methane and Gdm^+ ions is due to the characteristic hydration of Gdm^+ ions. The methanes are thus repelled from water to the location near the faces of Gdm^+ ions, in which the density of water molecules is relatively low (*vide supra*), leading to the lower first peak in the Me-O RDF in Fig. 4 (a).

Here we are interested in the correlations between the structure change in aqueous solutions upon salt additions and the effects of salts on the strength and dynamics of hydrophobic interactions. The effects of NH_4Cl result from the ability of NH_4^+ ions to form water structure in the vicinal region of methanes and reduce the structural fluctuation. The free energy difference between the SSM and the BARR is considered as the free energy cost of reformation of water structure around a methane dimer from the SSM to the BARR configuration. In this interpretation, NH_4^+ ions suppress the reformation of wa-

[1] The unclear peaks in the Me-Na^+ RDF may be partially attributed to the methane molecules being expressed in terms of spherically symmetric LJ model, while an analogous model in Ref. [12] shows a more distinct peak.

ter structure around a methane dimer, leading to the destabilization of the CM and BARR, and the stabilization of the SSM (See Fig. 1). The slower relaxation of the initial structure of the Me-Me DVH is thus owing to the suppression of reformation of water structure around a methane dimer.

The effects of GdmCl are related to the characteristic hydration of Gdm^+ ions. The Me-Me hydrophobic interaction is strongly enhanced in the large solvation shell surrounded by the planes of Gdm^+ ions bridged by water molecules and Cl^- ions as seen in Fig. 5. The ability of Gdm^+ ions to form large solvation shell is ascribed to their characteristic hydration, that is, their tendency of forming hydrogen bonds with water molecules and enhancing the structuring of water, and the hydrophobic like behavior of their planar faces. The more methane aggregation is enhanced, the larger the surface area of methane cluster becomes, thus water molecules having greater difficulty to form a solvation shell. Thus Gdm^+ ions assist methane clustering by forming the large solvation shell, resulting in the enhanced hydrophobic interaction and the extended lifetime thereof. Methanes can associate more loosely in the large solvation shell, leading to the outward movement of the CM, the BARR, and the SSM in the Me-Me PMF.

Urea and Gdm^+ ions have analogous salting-in and denaturing effects on amino acids [31,32] and proteins [33]. Soper et al. [34] have found that urea tends to form hydrogen bonds with itself, leading to large chains or cluster. Their and our results suggest that the similar effects of urea and Gdm^+ ions are due to their ability of forming large solvation shell and assisting the dehydration of hydrophobic molecules; they facilitate formation of empty molecular-sized cavities by excluding water molecules the vicinal region of hydrophobic molecules.

In the case of the effects of NaCl solution, we have not found significant correlations between the structure changes and the effects on the strength of hydrophobic interaction. Regarding the effects on the Me-Me DVH, the addition of NaCl has the smallest effects among the salts studied here (Fig. 2), which would be due to its little effects on the average water structure (see the O-O RDF in Fig. 3). The extension of the Me-Me association lifetime by NaCl may be associated with the reduction of water diffusivity. The absence of the contact peak in the $Me - Na^+$ RDF (Fig. 4 (b)) may play a role for the explanation, which remains to be elucidated.

4 Conclusion

We studied the effects of various salts on the strength and kinetics of hydrophobic interactions. The salts studied were sodium chloride, ammonium

chloride, and guanidinium chloride. Hydrophobic interaction is reduced by NH_4Cl ions, which results from their reduction of structural fluctuation, enhanced by GdmCl ions, the effect of which is ascribed to their ability of making large solvation shells, and slightly enhanced by NaCl, whose detailed mechanism remains to be elucidated. Concerning the dynamical aspect, we have found that the lifetime of hydrophobic associations is long in spite of their relatively weak interactions, which is considered as characteristic features of hydrophobic associations mainly due to the indirect effects of aqueous solutions. Addition of salts tends to extend the lifetime of hydrophobic associations by reducing water diffusivities and enhancing the structuring of water. The hydrophobic interactions upon salt additions are thus modified on a delicate balance due to the complex interplay of various molecular interactions.

Acknowledgement

The authors gratefully acknowledge the financial support provided by JST-CREST, and also thank Prof. Kuniyoshi Ebina for insightful comments.

References

[1] C. Tanford, The Hydrophobic Effect: Formation of Micelles and Biological Membranes, Wiley, New York, 1973.
[2] N.T. Southall, K.A. Dill, A.D.J. Haymet, J. Phys. Chem. B 106 (2002) 521.
[3] L.R. Pratt, Annu. Rev. Phys. Chem. 53 (2002) 409.
[4] G. Hummer, S. Garde, A.E. Jarcia, L.R. Pratt, Chem. Phys. 258 (2000) 349.
[5] K.D. Collins, M.W. Washabaugh, Q. Rev. Biophys. 4 (1985) 323.
[6] M.C. Cacace, E.M. Landau, J.J. Ramsden, Q. Rev. Biophys. 30 (1997) 241.
[7] S.N. Timasheff, Adv. Prot. Chem. 51 (1998) 355.
[8] P.E. Smith, J. Phys. Chem. B 103 (525).
[9] A. Karla, N. Tugen, S.M. Cramer, S. Garde, J. Phys. Chem. B 105 (2001) 6380.
[10] G. Hummer, S. Garde, A.E. Garcia, M.E. Paulaitis, L.R. Pratt, J. Phys. Chem. B 102 (1998) 10469.
[11] N.F.A. van der Vegt, W.F. van Gunsteren, J. Phys. Chem. B 108 (2004) 1056.
[12] T. Ghosh, A. Kalra, S. Garde, J. Phys. Chem. B 109 (2005) 642.
[13] M. Ikeguchi, S.K. Shimizu, J. Am. Chem. Soc. 123 (2001) 677.
[14] R.L. Mancera, Chem. Phys. Lett. 296 (1998) 459.
[15] P.H. Von Hippel, K-Y. Wong, Science 145 (1964) 577.
[16] H. Yang, A.H. Elcock, J. Am. Chem. Soc. 125 (2003) 13968.
[17] M.J. Dudek, J.W. Ponder, J. Comp. Chem. 16 (1995) 791.

[18] W.L. Jorgensen, J. Chandrasekhar, J.D. Madura, R.W. Impey, M.L. Klein, J. Chem. Phys. 79.
[19] E.M. Duffy, P.J. Kowalczyk, W.L. Jorgensen, J. Am. Chem. Sos. 115 (2003) 9271.
[20] R.C. Rizzo, W.L. Jorgensen, J. Am. Chem. Sos. 121 (1999) 4827.
[21] L. Verlet, J.J. Weis, Mol. Phys. 24 (1972) 1013.
[22] D. Beeman, J. Comput. Phys. 20 (1976) 130.
[23] T. Darden, D. York, L. Pedersen, J. Chem. Phys. 98 (1993) 952.
[24] H.J.C. Berendsen, J.P.M. Postma, W.F. van Gunsteren, A. DiNola, J.R. Haak, J. Chem. Phys. 81 (1984) 3684.
[25] N.T. Southall, K.A. Dill, Biophys. Chem. 101 (2002) 295.
[26] T. Ghosh, A.E. Garcia, S. Garde, J. Am. Chem. Soc. 123 (2001) 10997.
[27] P. Jund, W. Kob, R. Jullen, Phys. Rev. B 64 (2001) 134303.
[28] S. Kammerer, W. Kob, R, Schilling, Phys. Rev. E 58 (1998) 2141.
[29] P.E. Mason, G.W. Neilson, J.E. Enderby, M-L. Saboungi, C.E. Dempsey, A.D. MacKerell, J.W. Brady, J. Am. Chem. Soc. 126 (2004) 11462.
[30] P.E. Mason. C.E. Dempsey, G.W. Neilson, J.W. Brady, J. Phys. Chem. B 109 (2005) 24185.
[31] Y. Nozaki, C. Tanford, J. Biol. Chem. 238 (1963) 4074.
[32] Y. Nozaki, C. Tanford, J. Biol. Chem. 245 (1970) 1648.
[33] J.K. Myers, C.N. Pace, J.M. Scholtz, Protein Sci. 4 (1995) 2138.
[34] A.K. Soper, E.W. Castner, A. Luzar, Biophys. Chem. 105 (2003) 649.

Table 1
Number of species contained in the central periodic box for all the simulated systems

Salt	N_{water}	$N_{methane}$	N_{salt}	Salt Concentration (M)
None	515	10	0	0
NaCl	495	10	20	1.98
NH_4Cl	470	10	20	2.00
GdmCl	445	10	20	2.02

Table 2
Partial charges (q), Lennard-Jones interaction parameters (ϵ and σ) of various atom types used in MD Simulations. Lorentz-Berthelot mixing rules were used to model the Lennard-Jones interactions between species of different types.

Species	Atom	q/e	ϵ (kJ/mol)	σ (Å)
Water(TIP3P)	O	−0.834	0.6359	3.15
	H	0.417	0.0	0.0
Methane	Me	0.000	1.23	3.73
Na^+	Na^+	1.000	0.0116	3.33
NH_4^+	N	−0.400	0.7116	3.25
	H	0.350	0.0	0.0
Gdm^+	C	0.640	0.2039	2.25
	N	−0.800	0.7116	3.25
	H	0.460	0.0	0.0
Cl^-	Cl^-	−1.000	0.4939	4.41

Figure captions

Fig. 1. (a) Methane-methane pair potential of mean force, $W(r) = -k_B T \ln g(r)$, obtained from MD simulations at T=300 K in pure water (solid line), and aqueous solutions of NaCl (dashed line), NH_4Cl (dotted line), GdmCl (dash-dotted line). (b) Changes in the methane-methane PMF upon salt additions relative to the PMF in pure water, $\Delta W(r) = W(r) - W_{\mathrm{None}}(r)$.

Fig. 2. Methane-methane distinct part of van Hove correlation functions in pure water (a) and aqueous solutions of NaCl (b), NH_4Cl (c), GdmCl (d) at various t.

Fig. 3. (a) Radial distribution functions (RDFs) of water-water (O-O) in each system, the RDFs of (b) Na^+-water, (c) NH_4^+-water, and (d) Gdm^+-water, where molecular structure of Gdm^+ is also displayed.

Fig. 4. (a) Radial distribution functions (RDFs) of methane-water (O) in each system, and the RDFs of (b) methane-Na^+, (c) methane-NH_4^+, (d) methane-Gdm^+.

Fig. 5. A typical snapshot of large solvation shell assisting methane clustering. Green spheres represent chloride ions, and pink spheres represent methane solutes. Gdm^+ ions and water molecules are dipicted by spacefill and stick representations, respectively.

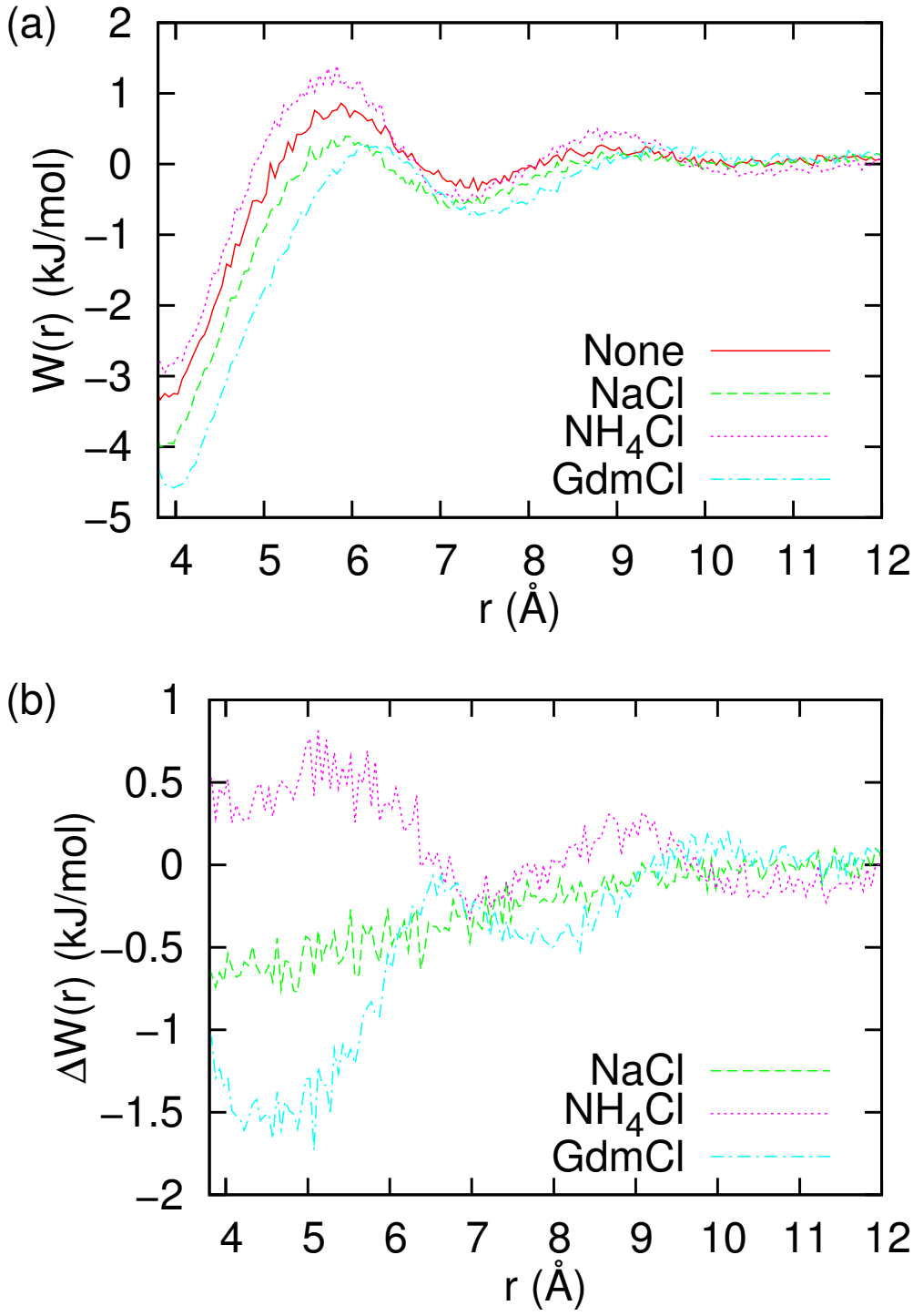

Fig. 1. (a) methane-methane pair potential of mean force, $W(r) = -k_B T \ln g(r)$, obtained from MD simulations at T=300 K in pure water (solid line), and aqueous solutions of NaCl (dashed line), NH_4Cl (dotted line), GdmCl (dash-dotted line). (b) Changes in the methane-methane PMF upon salt additions relative to the PMF in pure water, $\Delta W(r) = W(r) - W_{\mathrm{None}}(r)$.

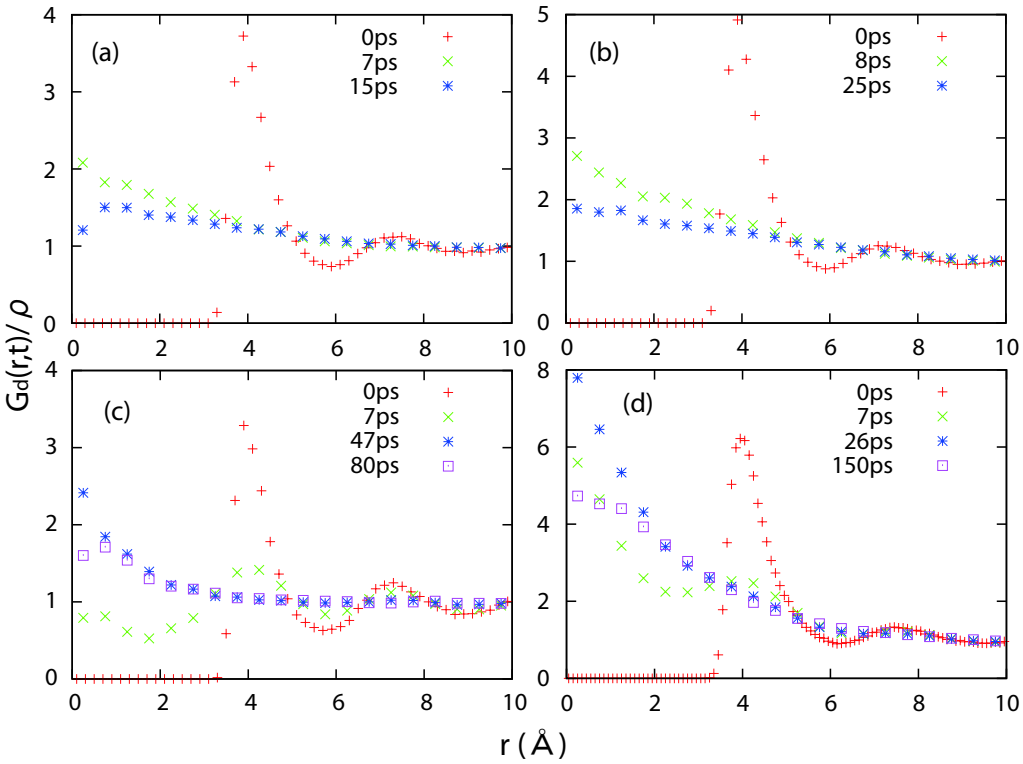

Fig. 2. Methane-methane distinct part of van Hove correlation functions in pure water (a) and aqueous solutions of (b) NaCl, (c) NH_4Cl, (d) GdmCl at various t.

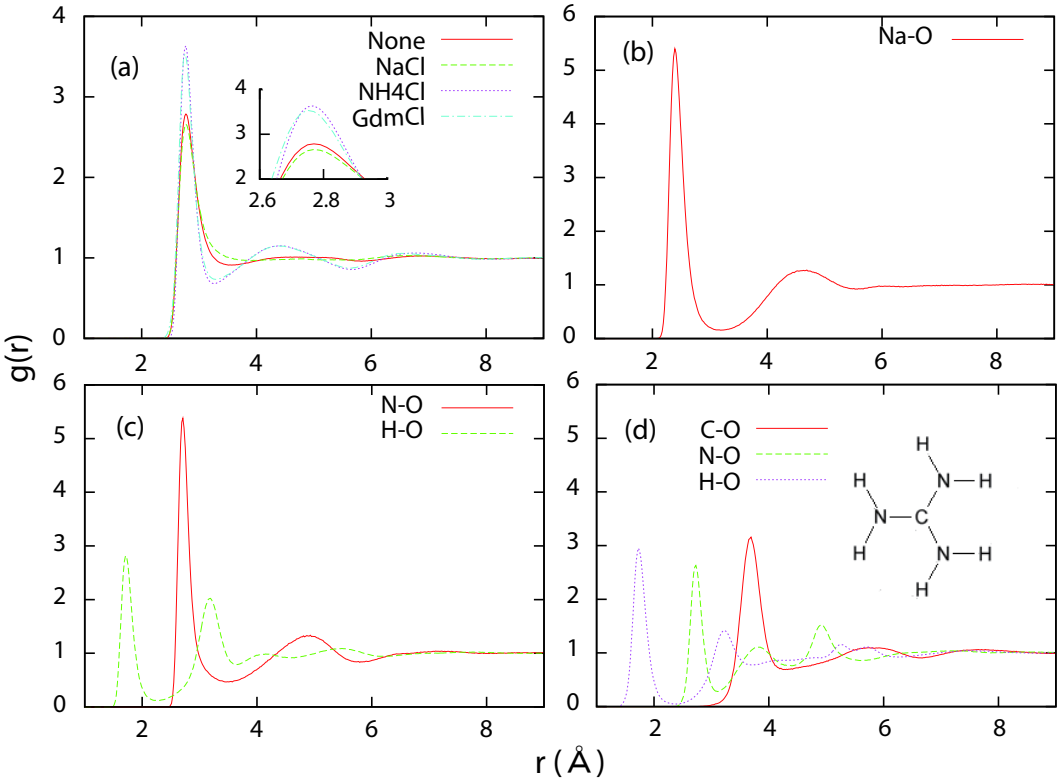

Fig. 3. (a) Radial distribution functions (RDFs) of water-water (O-O) in each system, the RDFs of (b) Na^+-water, (c) NH_4^+-water, and (d) Gdm^+-water, where molecular structure of Gdm^+ is also displayed.

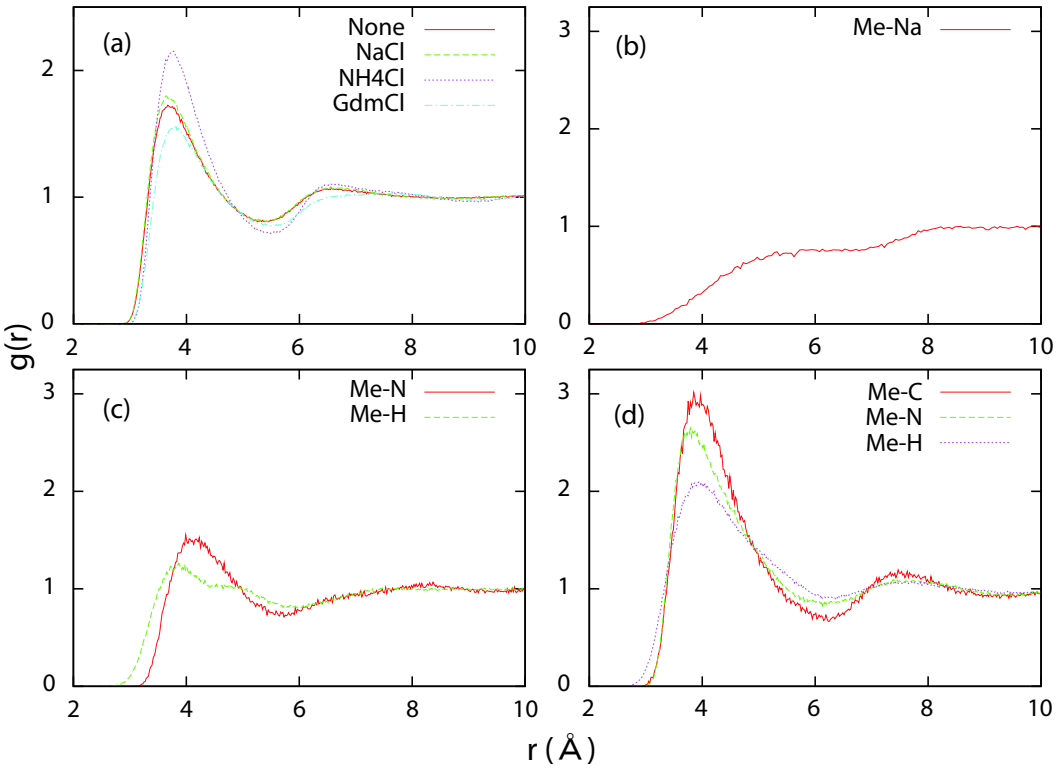

Fig. 4. (a) Radial distribution functions (RDFs) of methane-water (O) in each system, and the RDFs of (b) methane-Na^+, (c) methane-NH_4^+, (d) methane-Gdm^+.

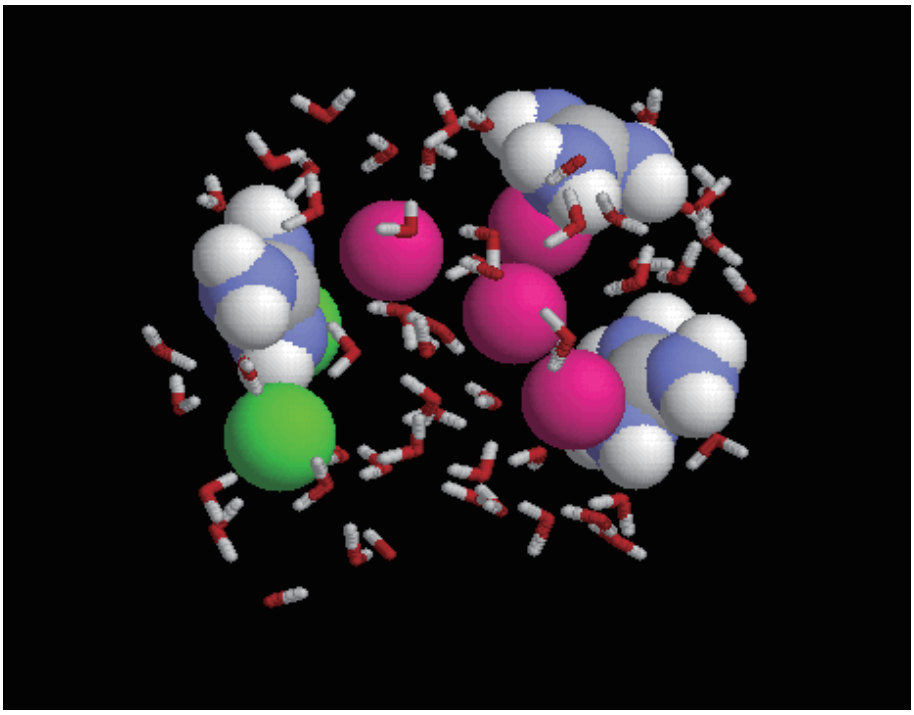

Fig. 5. A typical snapshot of large solvation shell assisting methane clustering. Green spheres represent chloride ions, and pink spheres represent methane solutes. Gdm^+ ions and water molecules are dipicted by spacefill and stick representations, respectively.